2016 IEEE PES Transmission & Distribution Conference and Exposition - Latin America (PES T&D-LA). Morelia, Mexico

Inertial Response of an Offshore Wind Power Plant with HVDC-VSC

V. Preciado, *Student Member*, V. Gevorgian*, Member, IEEE,*
E. Muljadi, *Fellow, IEEE,* M. Madrigal, *Senior Member*

***Abstract*—This paper analyzes the inertial response of an offshore wind power plant (WPP) to provide ancillary services to the power system grid. The WPP is connected to a high-voltage direct-current voltage source converter HVDC-VSC to deliver the power to the onshore substation. The wind turbine generator (WTG) used is a doubly-fed induction generator (Type 3 WTG).**

In this paper we analyze a control method for the WTGs in an offshore WPP to support the grid and contribute ancillary services to the power system network. Detailed time domain simulations will be conducted to show the transient behavior of the inertial response of an offshore WPP.

***Index Terms*--HVDC, inertial response, offshore wind turbine.**

I. INTRODUCTION

OFFSHORE WPPs will be more common in the next decades. Offshore wind power plants promise better wind resources than those onshore. Offshore WPPs tend to have higher average values and less turbulent winds. The distance of a WPP from the shore determines the type of power transmission to be implemented. It is generally accepted that for an offshore WPP located farther than 35 miles (56.33 kilometers), the economics of high-voltage direct-current (HVDC) operation are more attractive than those of high-voltage alternating-current transmission [1]. Fig. 1 depicts a typical HVDC system connected to an offshore WPP. Operation in variable-speed mode under HVDC has been documented [2-3]; however, the ancillary service functionalities are not included.

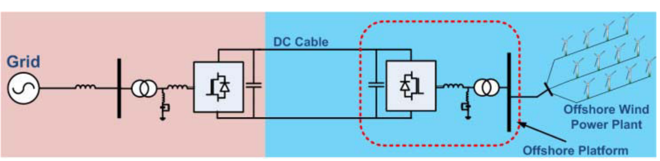

Fig. 1. A typical HVDC system connecting an offshore WPP to an onshore substation transformer

Modern WPPs have the ability to control active power output responding to grid frequency and this control ability can be important to support the grid performance in case of a sudden power generation loss [4].

E. Muljadi and V. Gevorgian are with National Renewable Energy Laboratory, Golden, CO, USA (Eduard_Muljadi@nrel.gov) and (Vahan.Gevorgian @nrel.gov)

V. Preciado and M. Madrigal are with Instituto Tecnologico de Morelia, Morelia, Michoacán, México. E-mail (preciado84@gmail.com) and (manuelmadrigal@ieee.org)

After the loss of a large power plant, it is usual to see that the grid frequency drops in the first seconds after the power loss. The frequency dynamics are initially dominated by the inertial response of the generators that remain online. The release into the grid of the kinetic energy stored in the synchronous generators reduces the initial rate of change of frequency (ROCOF) and allows slower governor actions to catch up and contribute to frequency stabilization. A performance similar to conventional generators can be achieved with a wind power plant by utilizing a controlled inertial response [5].

It is clear that the continuous growth of wind generation will have a big impact on the primary frequency system control. An analysis presented in [6] shows through numerous simulations that there is not a significant impact on the system frequency response due the reduction in system inertia because of higher levels of renewable generation when is compared with governor action in synchronous generators. Nevertheless, the application of controlled inertia response from wind power can help to increase the under-frequency load-shedding margin. Recent studies have shown that the frequency response in the United States, and especially in the Eastern Interconnection (EI), has been declining [7]. Reasons for this include high governor deadbands, generators operating in modes that do not offer frequency-responsive reserve (e.g., sliding pressure mode), governors that are not enabled, a reduced percentage of direct drive motor load, and many others [8-9].

The inertial response of a WPP depends on the electro-mechanical characteristics of each turbine inside the WPP, for the WTG Type 3, the rotor speed is decoupled of the grid frequency and this kind of turbine will exhibit inertial response if it is controlled for that purpose.

This paper shows an analysis of the transient behavior of an offshore WPP with an HVDC and will be organized in the following sequence. In Section II, the concept of HVDC voltage source converter (HVDC-VSC) operating mode is explained. In Section III, the inertial response of the offshore WPP is presented, Section IV presents the tests system used to simulate different conditions; in Section V simulations and results are presented for the discussion. Conclusion is presented in Section VI.

II. INERTIAL RESPONSE BASICS

Modern WPPs are required to operate like any other power plants to provide reliable power during normal operation and to support the grid during power system disturbances. The wind industry and the utility industry have good experience with normal operation of WPPs. The concept of WTG providing ancillary services is not new either [10-12]; however, the utilization of HVDC in an offshore WPP to provide ancillary services requires a previous analysis of the WPP inertial response.

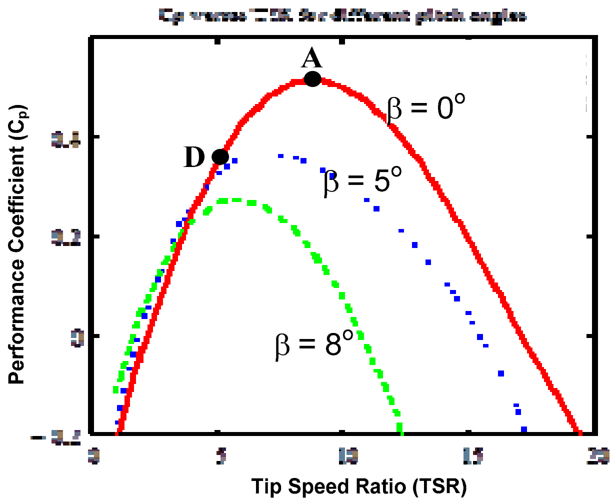

(a) Cp-TSR characteristic

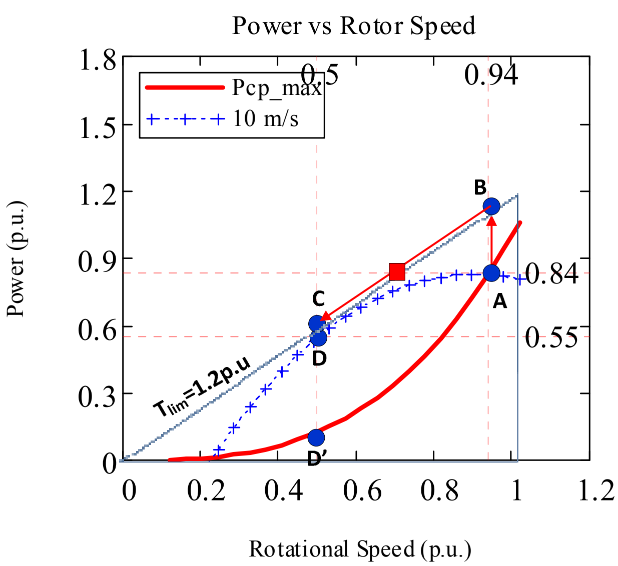

(b) Aerodynamic power and Generator Power

Fig. 2. Cp-TSR and the corresponding operating points

Fig. 2 illustrates the inertial response from a WTG. We presented the process and the operating points when a WTG release its kinetic energy during inertial response. Fig. 2a shows the performance coefficient or aerodynamic efficiency of a WTG as a function of tip-speed ratio. The corresponding operating points can be illustrated in Fig. 2b. Initially, the WTG operates in C_{pmax} operation. The aerodynamic operation is indicated as point A in the Cp-TSR characteristic shown in Fig. 2a. In the in C_{pmax} operation, the aerodynamic power stays at point A. The corresponding power-rotor speed characteristic is presented in Fig. 2b. When the WTG operates in C_{pmax} operation, the generator operating point and the aerodynamic power coincide as a single point moving along the thick red line where the power is a cubic function of the rotational speed. As the wind speed varies, the in C_{pmax} operation will move the generator and the aerodynamic operating points in synchrony along the thick red line.

Let's consider a WTG operating at wind speed of 10m/s. The aerodynamic power is indicated by the dash-blue line in Fig. 2b. The C_{pmax} operation is assumed and the operating points of both the generator power and the aerodynamic power coincide at point A. When all of a sudden, there is a request to deliver inertial response. The generator power is changed instantaneously by the power command delivered to the power converter. As a result, the generator operating moves from point A to point B. From the grid point of view, this sudden increase of output power ($\Delta P = P_B - P_A$) during frequency dip is viewed as the inertial response from WTG delivered to the grid. To make sure that the process does not creates too much stress on the gearbox, the generator torque is limited to torque limit of 120% (1.2 p.u.). The corresponding generator power is depicted as a linear blue line. Note, the light blue shading area represents a region of operation where the generator torque is allowed to operate (below torque limit). As the inertia of the rotating mass of the WTG blades, gearbox, generator, etc is very large, the rotational speed cannot change instantaneously. While the operating point of the generator moves from point A to point B, the operating point of aerodynamic of the WTG stays at point A. As $P_B > P_A$, the rotational speed decreases along the solid-blue line from point B to point C. Meanwhile, the aerodynamic power also moves from point A to point D as the rotor speed decreases. The corresponding aerodynamic characteristic as shown in Fig. 2a, also moving from point A to point D indicating that as the rotor speed slows down at constant wind speed, the aerodynamic efficiency slides down from C_{pmax}. Thus, the release of kinetic energy during the "forced slowdown" of the rotational speed is the inertial response of the WTG. The consequence of the release of kinetic energy is that the operating C_p of the WTG is less than the C_{pmax} (refer to Fig. 2a). At some point, say point C, the operating point of the generator is moved back to the C_{pmax} line (thick red line) from point C to point D'. As the generator output power is less than the aerodynamic power (P_D'< P_D). The rotational speed accelerates again moving the generator output power from P_D', and moving the aerodynamic power from P_D to meet the generator operating point at point P_A. Now, the WTG operates at C_{pmax} operation once again. The corresponding aerodynamic characteristics as shown in Fig. 2a, moves the operating point from D back to point A.

Although in this section one method of releasing kinetic energy is presented (the path ABCDA), there are many other methods used to control inertial response, and it is beyond the scope of the present paper.

III. Test System of an Offshore Wind Power Plant

A detailed 3-phase transient model of an offshore WPP consisting of several Type 3 2-MW wind turbines has been developed in Matlab™/Simulink™. The model uses 3-level IGBT based voltage source converter (VSC) topology for sending and receiving end terminals. Also, a buried XLPE export cable is used in the model. Both sending and receiving and VSC converters are set to DC-link voltage (+/- 100 kV DC) and reactive power control. The offshore collector system is modeled with the network of 33 kV XLPE cables. The conceptual diagram of the model is shown in Fig. 3.

The inertial response emulation control is a turbine–level control that allows injecting the kinetic energy of wind rotor mass in the grid to help reducing frequency rate of decline during contingencies.

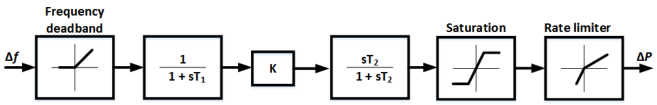

Fig. 3. Simplified inertial control model

TABLE I
PARAMETERS OF INERTIAL CONTROLLER

Parameter	Value used
Frequency deadband, p.u.	0.0025
Inertial controller gain K	10
Time constant T_1, sec	1
Time constant T_2, sec	5.5
Power signal saturation limits, p.u.	0.1
Rate limits, p.u./sec	+0.1; -1

In AC grid connected operation, the inertial response in individual turbines is triggered as soon as frequency decline is detected and frequency deviation from pre-fault level is above certain threshold. The inertial response is initiated by a torque (ΔT) or power (ΔP) command applied to the controller of power electronic converter. As a result, the DFIG's electromagnetic torque (T_{em}) increases, causing the turbine rotor to decelerate thus releasing its kinetic energy.

The simplified model of the inertial controller in accordance to [13] is shown in Fig. 3. This controller produces a power or torque order that is then applied to the turbine converter. The controller parameters used in simulations are shown in Table I. This set of parameters produces the power or torque order command as shown in Fig. 4. This particular shape of commanded torque is limited at 10% of turbine's rated value to reduce risks of excessive mechanical loads on turbine mechanical components. The parameters of the controller can be tuned to provide slightly different shapes of the torque command but still respecting the turbine safety limits.

Several simulations were conducted to analyze the dynamic behavior of the system shown in Fig. 4 when the average wind speed across the offshore WPP was around 12 m/s. The inertial response was triggered at different times depending on the conditions of each simulation.

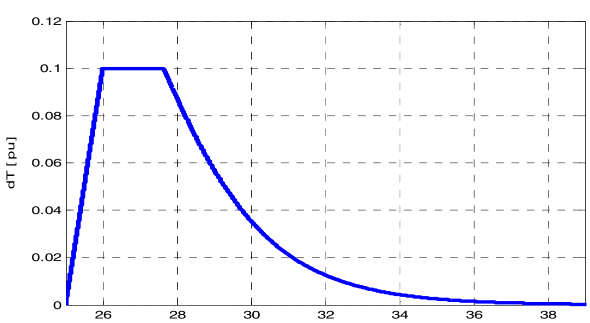

Fig. 4. ΔT order applied to the controller of the DFIG

Table II summarizes the simulations performed with different configuration conditions.

TABLE II
SIMULATIONS PERFORMED SUMMARY

Sim. No.	1	2	3
WTG	75	90	100
MW	150	180	200

IV. SIMULATION RESULTS AND DISCUSSION

In the study system shown in Fig. 5, an offshore wind farm (several turbines Type 3, 2 MW capacity per turbine) is connected to a 230kV, 60Hz 2500MVA equivalent system via an HVDC-VSC link 200MVA, ±100kV, 75 km long. Since the focus of the paper is on the inertial response of the offshore WPP, no automatic generator control (AGC) is included in the equivalent system connected to the inverter side of the HVDC link. The current-source DFIG wind farm model developed by GE [14] is used in this paper. The wind speed is assumed to be constant.

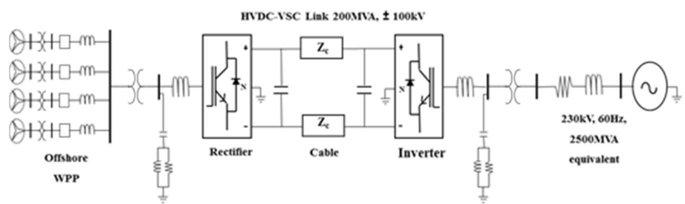

Fig. 5. Test system schematic

A. Simulation 1

The first case simulated consists of 75 WTG of 2 MW each, for a total capacity of 150 MW. The wind speed is assumed to be constant (12 m/s). In this case ΔT was applied at t = 25s (after the steady state was reached). Figs. 6 to 11 show the transient behavior for an HVDC 75 km long.

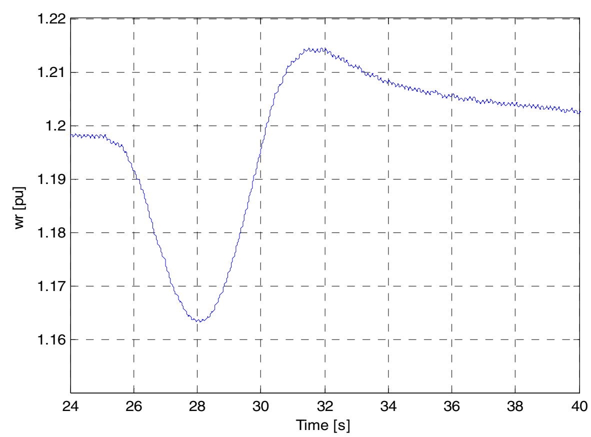

Fig. 6. DFIG rotating speed, 150 MW

As can be seen in Fig. 6, the DFIG rotational speed decreases when the ΔT is applied (at t=25s) as the electromagnetic torque in the machine is higher than the available aerodynamic power, Fig. 7. Also notice that the voltage in both sides of the HVDC link, Fig. 8, and also the HVDC link current, shown in Fig 9, increase when the torque command is applied, increasing (momentary) the power delivered to the grid by the offshore WPP.

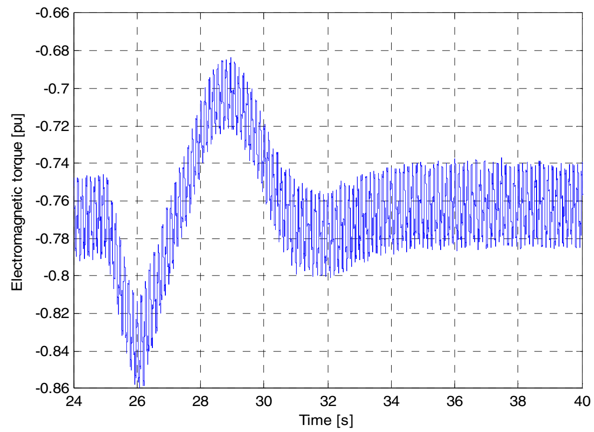

Fig. 7. DFIG electromagnetic torque, 150 MW

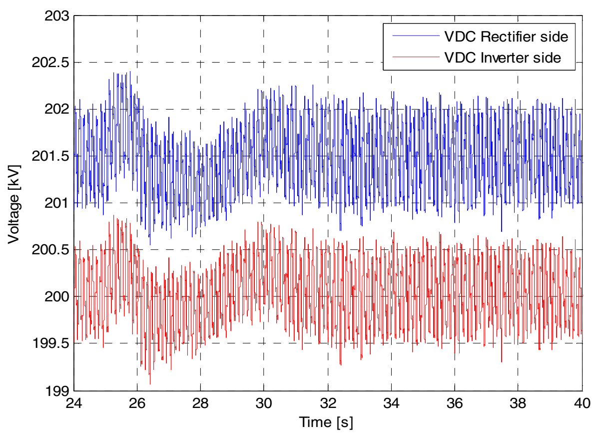

Fig. 8. HVDC link voltage , 150 MW

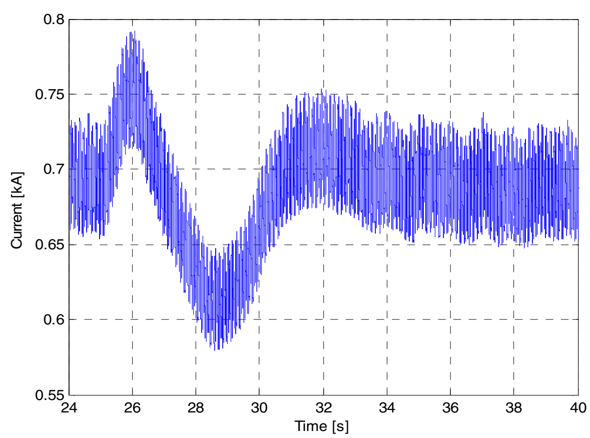

Fig. 9. HVDC link current, 150 MW

As ΔT represents a torque command caused by, for example, a major loss of generation that causes a frequency variation in the grid, the expected reaction from the WPP is to support the power in the grid delivering the kinetic energy from the turbine to the grid. The power delivered to the grid increases according to the torque pulse applied, as shown in Fig. 11.

The power delivered to the HVDC link by the offshore WPP is shown in Fig. 10, and as can be seen that it is stable at 150 MW and when ΔT is applied, the real power goes up to 160 MW, delivering the inertial response from the turbines to the grid and showing the typical transient behavior from an inertial response.

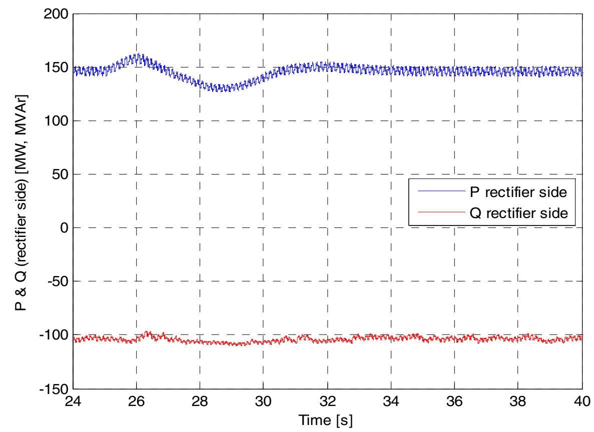

Fig. 10. Real and reactive power (rectifier side), 150 MW

A similar behavior is shown in Fig. 11, at the power delivered to the inverter side, 124 MW are delivered to the grid (due the losses in the cable), going up to 136 MW and showing that the HVDC link is capable to deliver a certain amount of extra power to the grid when it is requested.

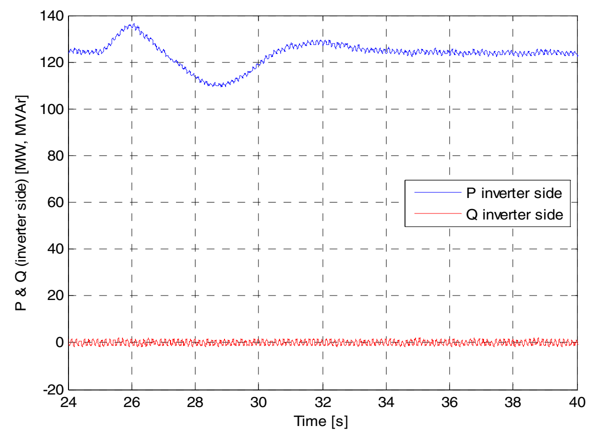

Fig. 11. Real and reactive power (inverter side), 150 MW

B. Simulation 2

The second case simulated consists of 90 WTG of 2 MW each, for a total capacity of 180 MW. The wind speed is also assumed to be constant (12 m/s). In this case ΔT was applied at t = 20 s (after the steady state was reached). Figs. 12 to 17 show the transient behavior for an HVDC 75 km long.

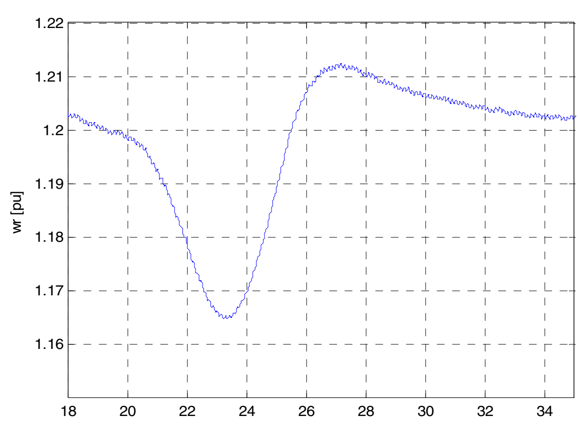

Fig. 12. DFIG rotating speed, 180 MW

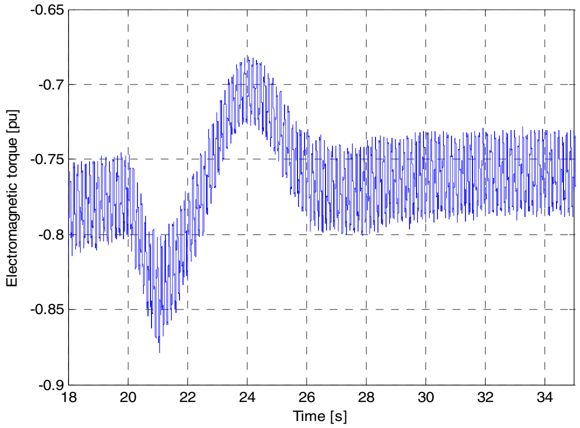

Fig. 13. DFIG electromagnetic torque, 180 MW

This case looks very similar to simulation 1, but attention must be paid to the fact that after the ΔT application (at t = 20s) the power sent from the wind turbines reaches momentarily the HVDC nominal capacity, the power sent goes up to 200 MW for a short period of time (1s), this is shown in Fig. 16.

Also should be noticed that the power injected to the grid (inverter side) shows a similar behavior, delivering around 150 MW to the grid before the torque pulse is applied, at t = 20s, the power delivered to the network increases to close to 160 MW, as can be seen in Fig. 17.

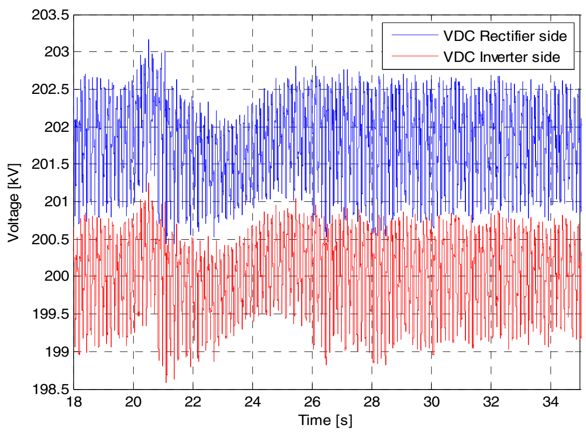

Fig. 14. HVDC link voltage , 180 MW

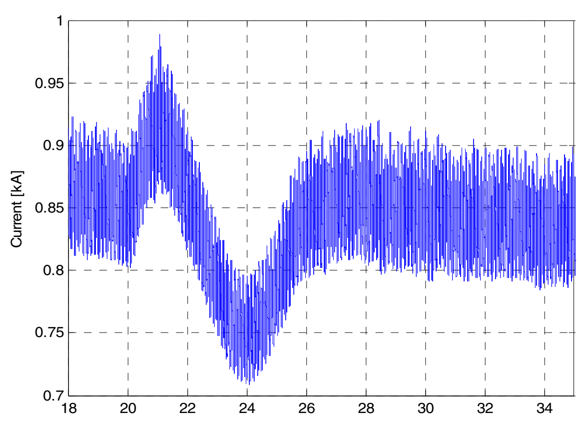

Fig. 15. HVDC link current, 180 MW

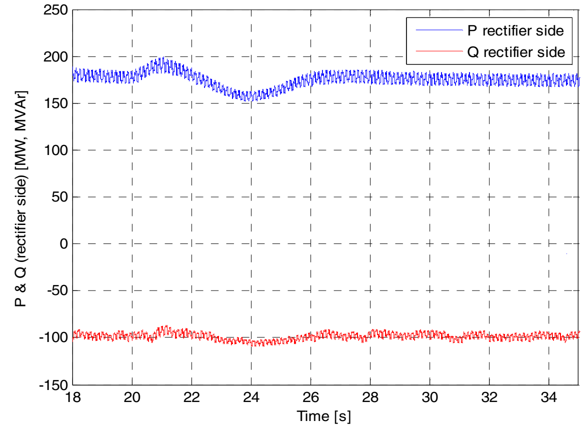

Fig. 16. Real and reactive power (rectifier side), 180 MW

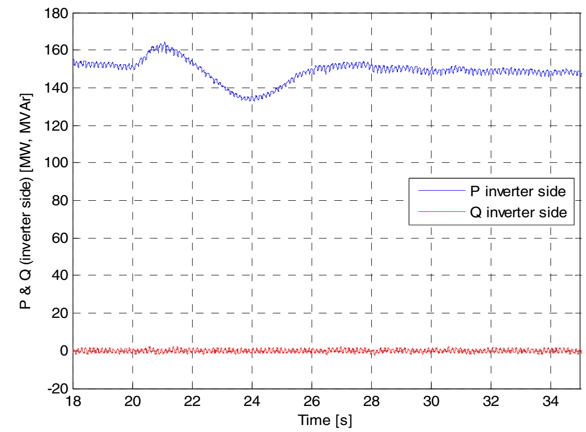

Fig. 17. Real and reactive power (inverter side), 180 MW

C. Simulation 3

Last case considered consists of 100 WTG of 2 MW each, for a total capacity of 200 MW to load the HVDC link at full capacity. In this case ΔT was applied at t = 20 s (after the steady state was reached). Figs. 18 to 21 show the transient behavior for an HVDC 75 km long with a wind speed of 12 m/s.

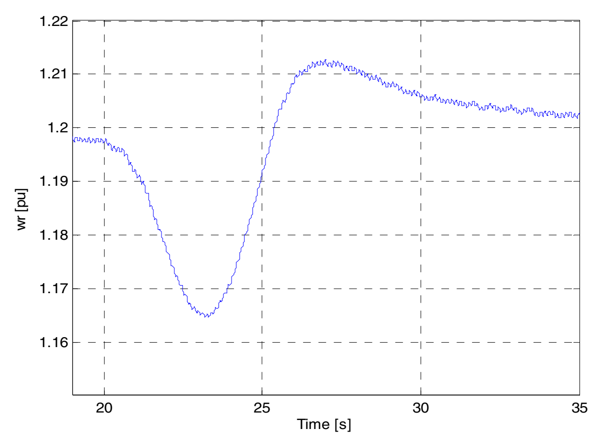

Fig. 18. DFIG rotating speed, 200 MW, 12 m/s

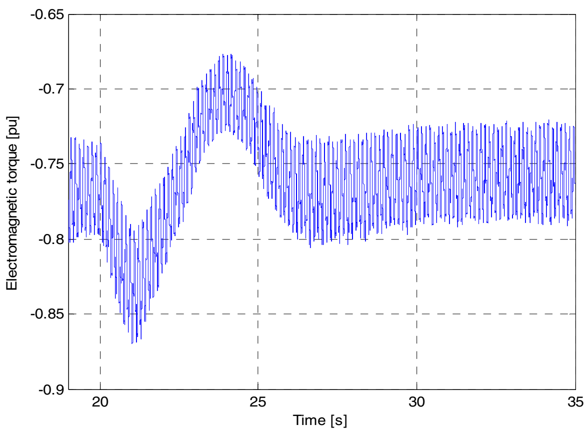

Fig. 19. DFIG electromagnetic torque, 200 MW, 12 m/s

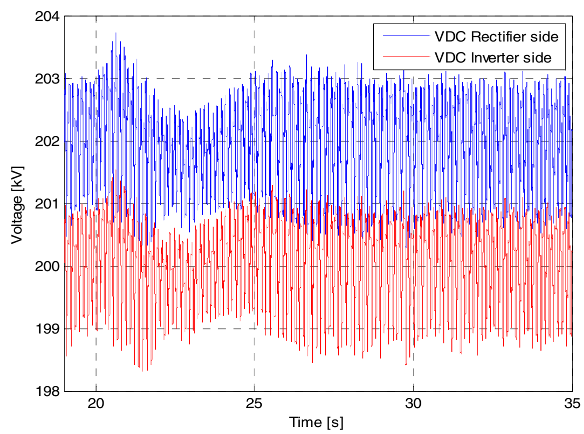

Fig. 20. HVDC link voltage , 200 MW, 12 m/s

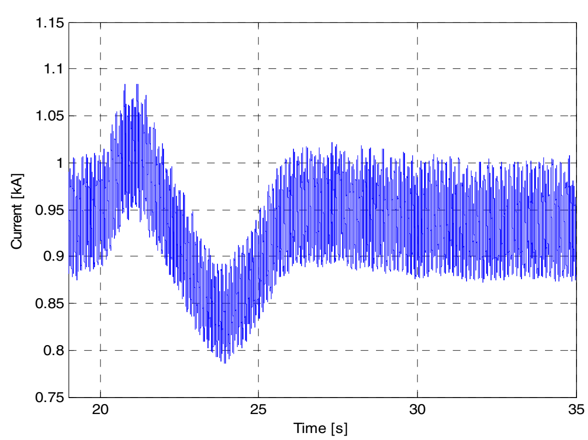

Fig. 21. HVDC link current, 200 MW, 12 m/s

As can be seen in Fig. 19, the electromagnetic torque varies according to the torque impulse applied and since is higher than the available aerodynamic power, generates an inertial response behavior in the system. Figs. 20 and 21 show the DC voltage (rectifier and inverter sides), the difference between both sides is around 1 kV which is related to the cable length. The voltage increases according to ΔT applied as well as the current flowing through the HVDC link, Fig. 21, to deliver the extra power required by the torque command.

The HVDC link works properly when the nominal power is sent through it. The first two seconds of the simulation the real power injected by the WPP is stable and at its rated value (200 MW), when the torque pulse is applied at t = 20s the power increases overloading momentarily the DC link; after the torque impulse is applied, the power increases to around 210 MW for a couple of seconds, following the behavior of the inertial response.

V. Conclusion

Detailed time domain simulations were conducted in order to analyze the transients present on the inertial response of an offshore WPP delivering power through an HVDC-VSC link.
Several results from transient behavior are presented, these results show that an offshore WPP connected to the grid via an HVDC-VSC link is able to deliver inertial response if it is requested.
These results are important as the WPP importance for the power system is growing and its performance during contingencies must be asured.

VI. References

[1] A. Bodin, “HVDC Light—A Preferable Power Transmission System for Renewable Energies.” Proceedings of the 2011 Third International Youth Conference on Energetics; July 7–9, 2011, Leiria, Portugal
[2] M. de Prada Gil, O. Gomis-Bellmunt, A. Sumper, and J. Bergas-Jané, “Analysis of a Multi-Turbine Offshore Wind Farm Connected to a Single Large Power Converter Operated with Variable Frequency.” Energy (36: 5), May 2011; pp. 3272–3281
[3] Feltes, C., and Erlich, I. “Variable Frequency Operation of DFIG-Based Wind Farms Connected to the Grid Through VSC-HVDC Link.” IEEE Power Engineering Society General Meeting, June 24–28, 2007, Tampa, Florida.
[4] N. Miller, K. Clark, M. Cardinal, and R. Delmerico, "Grid-friendly wind plants controls: GE WindCONTROL—Functionality and field tests," presented at European Wind Energy Conf., Brussels, Belgium, 2008.
[5] N. W. Miller, K. Clark, and M. Shao, “Impact of frequency responsive wind plant controls on grid performance,” presented at 9th International Workshop on Large-Scale Integration of Wind Power, Quebec, Canada, Oct. 18–19, 2010.
[6] N. Miller, M. Shao, and S. Venataraman, “California ISO: Frequency response study,” Final draft, Nov 9, 2011. Available at http://www.uwig.org/Report-FrequencyResponseStudy.pdf
[7] Ingleson, J.; Allen, E. “Tracking the Eastern Interconnection frequency governing characteristic.” Proceedings of the IEEE Power and Energy Society General Meeting; July 2010, Minneapolis, MN.
[8] Schulz, R. “Modeling of governing response in the Eastern Interconnection.” Proc. IEEE Power Engineering Society Winter Meeting; February 1999, New York, NY.
[9] Virmani, S. “Security impacts of changes in governor response.” Proc. IEEE Power Engineering Society Winter Meeting; February 1999, New York, NY.
[10] P.W. Christensen. G.T. Tarnowski.“Inertia of wind power plants – state of the art review year 2011”. 10th International Workshop on Large-Scale of Wind Power, Aarhus, Denmark, Oct 25-26, 2011.
[11] E. Muljadi, V. Gevorgian, M. Singh and S. Santoso, "Understanding Inertial and frequency Response of Wind Power Plants", IEEE PEMWA 2012, Denver CO, July 2012.
[12] Singh, M.; Gevorgian, V.; Muljadi, E.; Ela, E. (2013). Variable-Speed Wind Power Plant Operating With Reserve Power Capability: Preprint. 8 pp.; NREL Report No. CP-5500-58961.
[13] K. Clark, N. Miller, J.J. Sanchez-Gasca, “Modeling of GE wind-turbine generators for grid studies, version 4.5”, GE tech report, April 16, 2012.
[14] N. Miller, W. Price, and J. Sanchez-Gasca, “Modeling of GE wind turbine generators for grid studies,” General Electric International, Inc, Schenectady, New York, Tech. Rep., 2005.